Available online at www.sciencedirect.com
SCIENCE DIRECT®
International Journal of Heat and Mass Transfer 48 (2005) 317–329
International Journal of HEAT and MASS TRANSFER
www.elsevier.com/locate/ijhmt

New design equations for liquid/solid fluidized bed heat exchangers

M. Aghajani [a,b], H. Müller-Steinhagen [c,d,*], M. Jamialahmadi [b]

[a] Department of Chemical and Process Engineering, University of Surrey, Guildford, UK
[b] Petroleum University of Technology, Ahwaz, Iran
[c] Institute for Thermodynamics and Thermal Engineering, University of Stuttgart, Pfaffenwaldring 6, Stuttgart D-70550, Germany
[d] DLR Institute for Technical Thermodynamics, Stuttgart, Germany

Received 12 January 2004; received in revised form 4 August 2004

Abstract

Liquid/solid fluidized bed heat exchangers have originally been developed for desalination plants. However, due to their substantial benefits with respect to significantly improved heat transfer and fouling reduction, successful applications also exist in areas such as petrochemical, minerals and food processing as well as in the paper and power industries. The excellent performance of fluidized bed heat exchangers is related to the interaction between particles and heat transfer surface and to mixing effects in the viscous sublayer. In this paper, the results of experimental investigations on heat transfer for a wide range of Newtonian and non-Newtonian fluids are presented. New design equations have been developed for the prediction of bed voidage and heat transfer coefficients. The predictions of these correlations and of numerous correlations recommended by other authors are compared with a large database compiled from the literature.

Keywords: Liquid/solid fluidized beds; Non-Newtonian fluid; Heat transfer; Bed voidage; Correlations

1. Introduction

Liquid/solid fluidized beds are used throughout the process industry for hydrometallurgical operations, catalytic cracking, crystallization and sedimentation. In addition to the excellent mixing of the bulk fluid, significant increase in heat transfer up to a factor of 8 has been observed due to the presence of the suspended particles, Jamialahmadi and Müller-Steinhagen [1]. A further advantage is the scouring action of the particles, which may greatly reduce the formation of deposits on the heat transfer surfaces, Müller-Steinhagen [2]. Therefore, fluidized bed heat exchangers with cylindrical stainless steel particles as solid phase have been recommended for processes where severe fouling of the heat transfer surfaces is expected, Klaren [3]. An example of such a heat exchanger is shown in Fig. 1.

Typical installations for this technology are desalination plants, geothermal plants, paper mills, refineries etc. In recent years, solid–liquid fluidized beds are also finding increasing applications in treatment of aqueous wastes, heavy oil cracking, polymerisation, biotechnology,

* Corresponding author. Address: Institute for Thermodynamics and Thermal Engineering, University of Stuttgart, Pfaffenwaldring 6, Stuttgart D-70550, Germany. Tel.: +49 711 685 3536; fax: +49 711 685 3503.
E-mail address: hms@itw.uni-stuttgart.de (H. Müller-Steinhagen).

0017-9310/$ - see front matter © 2004 Elsevier Ltd. All rights reserved.
doi:10.1016/j.ijheatmasstransfer.2004.08.008

Nomenclature

A_c	surface area affected by forced convection (m^2)
A_p	surface area affected by particles (m^2)
a–f	coefficients and exponents
C_D	drag coefficient
C_P	heat capacity (J/kg K)
d_b	bubble diameter (m)
d_p	particle diameter (m)
D	diameter of fluidized bed (m)
D_h	hydraulic diameter of fluidized bed (m)
f	collision frequency (s^{-1})
f_i	friction factor
K	constant
n	Richardson and Zaki exponent
$\dot{q}$	heat flux (W/m^2)
T	temperature (K)
t	time (s)
u_s	superficial liquid velocity (m/s)
u_t	particle terminal velocity corrected for wall effect (m/s)
u_∞	particle terminal velocity in an infinite fluid (m/s)
X	length in flow direction (m)
z	fluidization index

Greek letters

α	heat transfer coefficient ($W/m^2 K$)
ε	bed voidage
λ	thermal conductivity (W/m K)
μ	dynamic viscosity (kg/m s)
σ	standard deviation
ρ	density (kg/m^3)
τ	shear stress (Pa s)
Ψ	shape factor
$\dot{\gamma}$	shear rate (s^{-1})
μ_a	apparent viscosity (kg/m s)

Subscripts–superscripts

a	apparent
av	average
b	bulk
c	forced convection
c	contact
D	drag
f	fluid
l	liquid
p	particle
s	solid
SB	static bed
w	wall
wl	wall to adjacent liquid
wp	wall to the particle
∞	infinity

Dimensionless groups

Ar	Archimedes number, $gd_P^3(\rho_s - \rho_l)\rho_l/\mu_l^2$
Nu	Nusselt number, $D\alpha/\lambda_l$
Pr	Prandtl number, $\mu_l C_{pl}/\lambda_l$
Re	Reynolds number, $\rho_l u_s D/\mu_l$
Re_p	particle Reynolds number, $\rho_l u_s d_P/\mu_l$
$Re_{p\infty}$	particle terminal Reynolds number in an infinite liquid, $\rho_l u_\infty d_P/\mu_l$

fermentation, and food processing. Here, the liquid phase is viscous with non-Newtonian behaviour.

To apply fluidized bed heat exchangers more widely, one has to be able to predict the heat transfer coefficient for a given condition through the knowledge and understanding of the mechanisms involved. Investigations on the hydrodynamic behaviour of Newtonian systems have been documented and discussed by Jamialahmadi and Müller-Steinhagen [1]. This work has now been extended to cover hydrodynamics and heat transfer of Newtonian and non-Newtonian fluids with particles of a wide range of sizes, shapes and densities, Aghajani [4].

2. Experimental set-up

2.1. Test rig for measuring heat transfer coefficients

A schematic diagram of the apparatus used in this investigation is shown in Fig. 2. The test rig was completely made from stainless steel. The liquid flows in a closed loop consisting of temperature controlled storage tank, pump, liquid flow meter, control valves, and the electrically heated test section, which is a vertical tube with an inner diameter of 25.4 mm (see Fig. 3).

A 70-mesh stainless steel screen fitted between two flanges before the test section supports the solid particles. The fluid temperature in the test section was measured with appropriately installed thermocouples. The flow meter was calibrated for different solutions at different bulk temperatures. The particles were prevented from carryover, at higher superficial liquid velocities, by an expansion cone mounted on top of the heated section. Power was supplied to the test section using a manually adjusted variac. A personal computer was used for data acquisition. Various types of spherical and cylindrical particles were used as solid phase in this investigation.

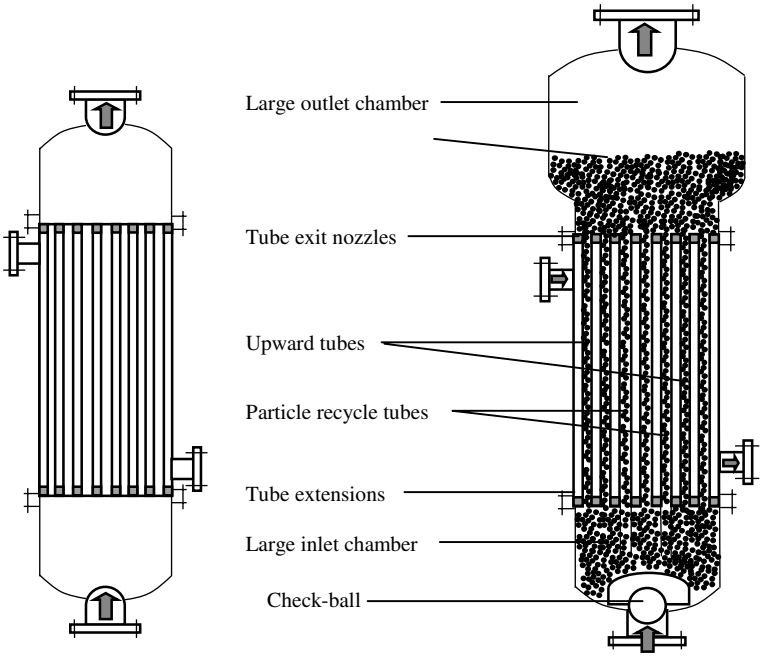

Fig. 1. Conventional heat exchanger and modified heat exchanger with circulating fluidized bed.

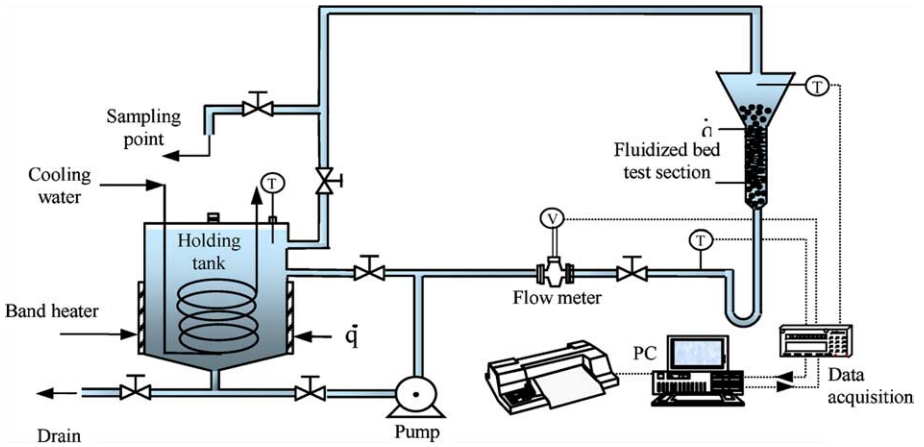

Fig. 2. Schematic diagram of test apparatus.

The local heat transfer coefficient is defined as:

$$\alpha = \frac{\dot{q}}{T_s - T_b} \tag{1}$$

where the surface temperature, T_s, is calculated as shown in the previous section. The local bulk temperature, T_b, at the wall thermocouple location was obtained from the inlet and outlet temperatures of the test section using the following equation to account for the heater geometry.

$$T_b = T_{b,in} + \frac{95}{160}(T_{b,out} - T_{b,in}) \tag{2}$$

Assuming that the bulk temperature increases linearly, from $T_{b,in}$, to $T_{b,out}$ of the heated section is a valid assumption for constant heat flux boundary condition. Experiments for measuring heat transfer coefficients were performed for different bulk temperatures. All measurements were taken after the system had reached steady state conditions.

From the results of this study and also from previous investigations it has been found that in the convective heat transfer regime, the heat transfer coefficient is almost independent of the heat flux. Therefore, to perform all experiments under identical operational conditions

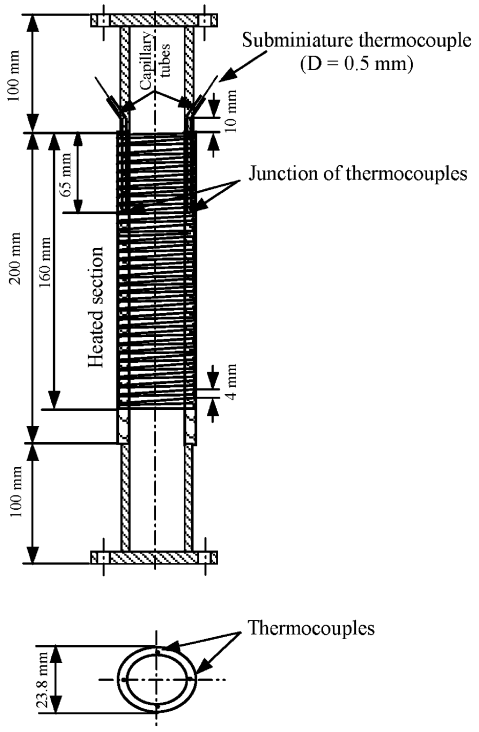

Fig. 3. Schematic of fluidized bed test section.

and to remain in the convective heat transfer regime, the heat flux was maintained at 57 kW/m^2, if the test liquid is pure water or a sugar solution. Because of the high viscosity of test liquids in the experiments with CMC solution, the heat flux was then maintained at 25 kW/m^2 to avoid overheating and deposit formation. The range of experimental parameters used for measuring heat transfer coefficients is given in Table 1.

Table 1
Range of experimental parameters for the measurements of heat transfer coefficients

d_p/D_h	0.0013–0.265
ρ_P	2290-11,350 kg/m^3
ρ_l	816–1324 kg/m^3
μ_l	0.0003–0.5220 Pa s
Re_p	0.019–11,302
Ar	3.85–6.1 × 10^7
Pr	1.55–7687

2.2. Investigated particles and liquids

Various types of spherical and cylindrical particles were used as solid phase, with physical properties listed in Table 2. In order to cover a wide range of particle Reynolds numbers, a series of aqueous solutions of sugar and carboxymethylcellulose (CMC) were used as Newtonian and non-Newtonian liquids. The concentration of sugar and CMC was varied from 0 to 60 wt.% and 0 to 1 wt.% respectively. The sugar solutions exhibited a constant shear viscosity, whereas the CMC solutions displayed varying levels of pseudo-plastic behaviour. An examination of the steady shear stress-shear rate data suggested that the two-parameter power law fluid model provides an adequate representation of their pseudo-plastic behaviour. For steady shear, the power law is written as:

$$\tau = k\dot{\gamma}^n \tag{3}$$

Table 2
Physical properties of solid particles

Type	Name	d_p or d_{pe}[a] [mm]	ε_{SB}	Ψ	Density [kg/m^3]	Specific heat [J/kg K]	Conductivity [W/m K]
Cylindrical	Aluminium 2 × 3 mm	2.62	0.40	0.86	2600	896	204
	Aluminium 3 × 3 mm	3.43	0.41	0.87	2600	896	204
	Brass 3 × 3 mm	3.43	0.41	0.87	8500	385	111
	Stainless Steel 3 × 3 mm	3.43	0.41	0.87	7900	460	17
	Stainless Steel 2 × 2 mm	2.29	0.40	0.87	7900	460	17
	Tantalum 4 × 4 mm	4.58	0.41	0.87	17,600	151	54.4
Spherical	Glass	2	0.39	1	2700	840	0.87
	Glass	3	0.39	1	2700	840	0.87
	Glass	4	0.40	1	2700	840	0.87
	Lead	2.9	0.39	1	11,350	130	35
	Lead	4	0.40	1	11,350	130	35
	Carbon Steel	4	0.40	1	7800	473	43
	Carbon Steel	3	0.39	1	7800	473	43
	Stainless Steel	3.7	0.40	1	8100	460	13

[a] d_{pe} = Equivalent diameter for cylindrical particle = diameter of a sphere having the same volume as the particle (volume diameter).

Table 3
Physical properties of test liquids

Newtonian liquids	Viscosity [Pa s]				Density [kg/m^3]	Specific heat [J/kg K]	Conductivity [W/m K]
	25 °C	40 °C	60 °C	80 °C			
Pure water	0.0010050	0.0006560	0.0004688	0.0003565	998.3	4182	0.6
Sugar solutions						_[a]	_[a]
20 wt.%	0.001714	0.001197	0.000811	0.000592	1070	1523	0.580
40 wt.%	0.005359	0.003261	0.001989	0.001339	1150	1314	0.456
60 wt.%	0.044410	0.021300	0.009870	0.005420	1300	1184	0.391

Aqueous solutions of CMC (non-Newtonian liquids)
Density ≅ density of pure water
Power law model: $\tau = k(\dot{\gamma})^n$ where k = viscosity coefficient, [Pa s^n] and n = rate index

CMC solutions	Power law parameters	25 °C	40 °C	50 °C	60 °C	70 °C	Specific heat [J/kg K]	Conductivity [W/m K]
0.2 wt.%	k	0.0697	0.0221	0.0125	0.0082	0.0031	4200	0.615
	n	0.7468	0.8281	0.8879	0.9233	0.9512		
0.4 wt.%	k	0.2084	0.066078	0.03737	0.02452	0.00927	4220	0.625
	n	0.6953	0.770993	0.82667	0.85963	0.8856		
0.6 wt.%	k	0.3413	0.108217	0.06121	0.04015	0.01518	4250	0.635
	n	0.6883	0.763231	0.81835	0.85097	0.87669		
0.8 wt.%	k	0.5756	0.182507	0.10323	0.06772	0.0256	4270	0.64
	n	0.6729	0.746155	0.8012	0.83193	0.85707		
1 wt.%	k	2.538	0.804732	0.45516	0.29859	0.11288	4290	0.645
	n	0.5519	0.611982	0.65618	0.68234	0.70296		

[a] International Critical Tables, Vol. 5, 1929.

where the best values of k and n were estimated using a non-linear regression approach. The resulting values along with the density of each solution are given in Table 3. It has been assumed that the average shear rate over the entire particle surface is u_∞/d_p. With this definition, the apparent viscosity is given by the following equation:

$$\mu_a = k\left(\frac{u_\infty}{d_p}\right)^{n-1} \tag{4}$$

3. Results and discussion

3.1. Velocity–voidage relationship

Correlations available for the prediction of heat transfer coefficients are strong functions of the bed voidage. Therefore, accurate knowledge of this parameter is crucial for the reliable estimation of transfer coefficients. Jamialahmadi and Müller-Steinhagen [5] compiled the published correlations and conditions for which their application has been recommended. Most correlations are empirical and apply only over a restricted range of Reynolds numbers, for specific particles and usually for Newtonian fluids. Therefore, a new model has been suggested by Aghajani [4]:

$$\varepsilon = \left(\frac{u_s}{u_t}\right)^{1/z}(1-\varepsilon_{SB}) + \varepsilon_{SB} \tag{5}$$

The static bed voidage ε_{SB} in Eq. (5) can be calculated by the following equations:

– for spherical particles

$$\varepsilon_{SB} = \frac{0.15}{\left(\frac{D_h}{d_p}-1\right)} + 0.38; \quad \frac{D_h}{d_p} \geqslant 2.033 \tag{6}$$

– for cylindrical particles

$$\varepsilon_{SB} = \frac{0.15}{\left(\frac{D_h}{d_p}-1\right)} + 0.39; \quad \frac{D_h}{d_p} \geqslant 2.033 \tag{7}$$

The fluidization index, z, can be calculated by the following equation:

$$z = \frac{0.65(2+0.5Re_{p\infty}^{0.65})}{(1+0.5Re_{p\infty}^{0.65})} \tag{8}$$

Eq. (8) is independent of the nature of the fluids and it can equally well be used for Newtonian and non-Newtonian liquids. The nature of the fluid is taken into consideration by using the apparent viscosity in the calculation of parameters such as the Archimedes number and the particle Reynolds number.

The predictions of the above model have been compared to a large data base with more than 1000 data from the literature and from own measurements. For Newtonian liquids, an average error of 6.18% and for non-Newtonian (shear-thinning power law) fluids an average error of 6.95% has been achieved. This is demonstrated in Fig. 4 for the experimental data of different investigators. Most published correlations for the bed voidage vs. velocity relationship have also been compared with the data base of Aghajani [4]. From this group, the correlation of Hartman et al. [16] performed best for Newtonian liquids (5.79% average error), while the correlation of Letan [18] achieved an average error of 8.61% for non-Newtonian liquids. However, none of the published correlations outperformed the equation presented above for the whole range of fluids.

3.2. Particle terminal velocity corrected for wall effect

Particle settling velocity is essential for the prediction of bed voidage, heat and mass transfer coefficients. It is well known that the walls of the column exert an additional retardation effect on a settling solid particle. The extent of this wall effect is usually quantified by introducing a wall factor defined as:

$$f = \frac{\text{Terminal settling velocity in the presence of wall effect}}{\text{Terminal settling velocity in the absence of wall effect}} = \frac{u_t}{u_\infty}$$

It is obvious that f has a positive value less than 1. From the work of Aghajani [4] it was found that the following equation proposed by Richardson and Zaki [8] is very well suited for calculating particle terminal velocity corrected for wall effect:

$$\mathrm{Log}_{10}\left(\frac{u_\infty}{u_t}\right) = \frac{d_p}{D_h} \tag{9}$$

3.3. Correlations for particle free fall velocity

The forces acting on a particle moving with its terminal velocity through a fluid are in dynamic equilibrium. Namely, the effective weight (gravitational force minus buoyancy force) is equal to the drag force. For the free fall terminal velocity this leads to:

$$u_\infty = \sqrt{\frac{4d_p(\rho_p - \rho_l)g}{3C_D\rho_l}} \tag{10}$$

Eq. (10) may be written in terms of free fall particle Reynolds number:

$$Re_{p\infty} = \sqrt{\frac{4\rho_l d_p^3(\rho_p - \rho_l)g}{3C_D\mu^2}} \tag{11}$$

Eq. (11) shows that the terminal velocity of a particle is inversely proportional to the drag coefficient, C_D. Theoretically, the drag coefficient can be obtained from the

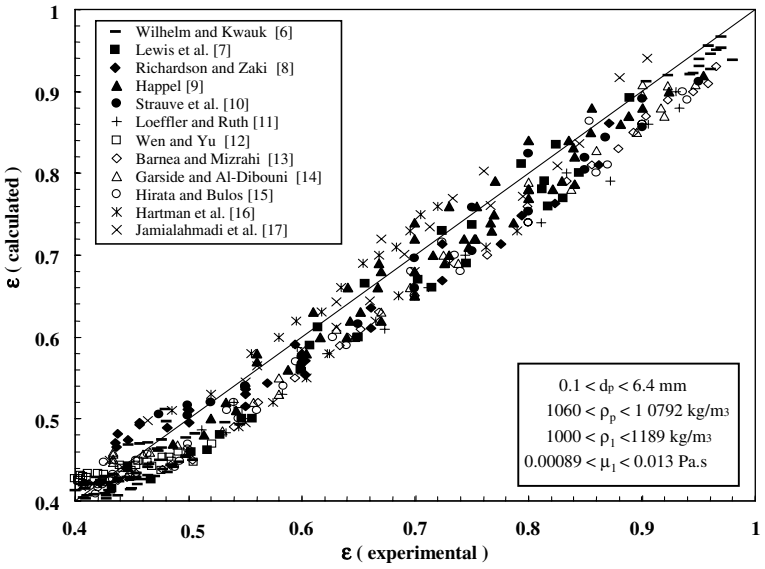

Fig. 4. Comparison of measured bed voidages with values calculated from Eq. (5) for Newtonian and non-Newtonian solutions [6–17].

solution of the equation of momentum for the system. In the absence of inertial terms it yields:

$$C_D = \frac{24}{Re_{p\infty}} \tag{12}$$

As the particle Reynolds number increases, the inertial terms become increasingly significant in the momentum equation and no analytical solutions are possible under these conditions. Therefore, almost all drag coefficients reported for higher Reynolds number have been obtained from experiments. These results are generally presented in graphical form as a complex function of the flow conditions. Most of this work has been reviewed and critically evaluated by several investigators [19,20]. Unfortunately, the form of these correlations is not convenient for the calculation of the free settling velocity for a given solid–liquid system as the unknown velocity appears in both $Re_{p\infty}$ and C_D. This difficulty is overcome by writing Eq. (11) in terms of Archimedes number, which is not a function of the terminal velocity:

$$Ar = \frac{3}{4} C_D Re_{p\infty}^2 = \frac{g\rho_l(\rho_p - \rho_l)d_p^3}{\mu^2} \tag{13}$$

Eq. (13) shows that the particle free fall Reynolds number is only a function of Archimedes number and can be better presented in the form:

$$Re_{p\infty} = F(Ar) \tag{14}$$

Several attempts have been made to establish the functionality between the Archimedes number and the particle Reynolds number. Most of this work is documented and critically evaluated by Khan and Richardson [20].

Hartman et al. [21] proposed the following explicit relation for the prediction of the free fall velocity of a spherical particle in an infinite medium. According to Aghajani [4], this is presently the best available correlation for calculating $Re_{p\infty}$ for Newtonian solutions:

$$\mathrm{Log}_{10} Re_{p\infty} = P(C) + \log_{10} R(C) \tag{15}$$

where

$$P(C) = ((0.0017795C - 0.0573)C + 1.0315)C - 1.26222$$
$$R(C) = 0.99947 + 0.01853 \sin(1.848C - 3.14) \tag{16}$$

and

$$C = \mathrm{Log}_{10} Ar \tag{17}$$

Few attempts have been made to establish the functional dependence of Archimedes number on particle Reynolds number for solutions with non-Newtonian flow behaviour. Aghajani [4] determined improved values for the constants in Eq. (14), by non-linear regression analysis of all published data available at the time:

$$Re_{p\infty} = 0.334 Ar^{0.654} \tag{18}$$

For non-Newtonian solutions, the apparent viscosity, μ_a, must be used in both, $Re_{p\infty}$ and Ar. Therefore, Eq. (18) is implicit with respect to the free particle terminal settling velocity, u_∞, and must be solved in parallel with Eq. (10). Eq. (18) predicts the free fall velocity of particles in non-Newtonian solutions with an absolute mean average error of less than 10%.

3.4. Heat transfer

Heat transfer to/from solid/liquid fluidized beds must be influenced by the intensity of the interchange between the solid particles and the heater surface, which is a function of the velocity of the particles and the frequency and density of particle contact with the heater surface. Hence, a new model has been formulated based on the following assumptions:

(1) The major resistance to heat transfer is a liquid film near the heat transfer surface.
(2) Due to the movement of solid particles there is a steady flow of fluid elements from the bulk of the fluid to the heat transfer surface and vice versa. The fluid elements reside for a finite time at the surface until they return to the bulk in the wake of solid particles scouring the heat transfer surface. In this region heat is transferred into the fluid by transient heat conduction from the heat transfer surface. Some heat is also transferred by conduction to the particles while they are in contact with the heat transfer surface.
(3) On sections of the heat transfer surface that are not in contact with particles, heat is transferred to the liquid by forced convection.

Therefore heat transfer at any moment is composed of two parallel mechanisms in separate zones of the heat transfer surface, i.e. the surface area affected by particles, A_p, and the remaining heat transfer area, A_c, in which heat is transferred by forced convection.

Han and Griffith [22] have shown that the area from which the hot liquid layer is pumped away by a vapour bubble leaving the heat transfer surface is πd_b^2. Since small bubbles and solid particles behave similarly, the area of the heat transfer surface affected by a single particle should also be πd_p^2. The following approach is hence analogous to nucleate boiling heat transfer if "vapour bubble" is replaced by "particle" and "latent heat transfer" by "particle conduction".

Time-averaged heat transfer coefficients may be additive if it is assumed that both mechanisms (heat transfer by fluid convection and heat transfer by transient heat conduction from the heat transfer surface) coexist over the entire heat transfer surface. Therefore, the total heat transfer coefficient α is

$$\alpha = \alpha_c + \alpha_p \tag{19}$$

The local forced convective heat transfer coefficient, α_c, can be calculated from the Gnielinski [23] equation for heat transfer during turbulent flow in pipes if it is modified to apply for local conditions.

$$Nu = \frac{\frac{f_i}{8}(Re - 1000)Pr}{1 + 12.7\sqrt{\frac{f_i}{8}}(Pr^{2/3} - 1)}\left[1 + \frac{1}{3}\left(\frac{D}{X}\right)^{2/3}\right]\left(\frac{Pr_b}{Pr_w}\right)^{0.11} \tag{20}$$

Based on extensive experimental and numerical research Jamialahmadi and Müller-Steinhagen [5] suggested to use Re instead of $(Re - 1000)$ in Eq. (20), which was also adopted for the present work. The friction factor, f_i for turbulent flow may be calculated according to Filonenko [24].

$$f_i = [1.82\mathrm{Log}(Re) - 1.64]^{-2} \tag{21}$$

An average relative error of 5.7% for Newtonian solutions and 8.6% for non-Newtonian (shear-thinning power law) solutions confirms the good agreement between the measured single-phase data and the predictions of the modified Gnielinski [23] equation.

3.5. Prediction of α_p

The heat transfer coefficient for the particle-controlled area, α_p also includes two parallel heat transfer coefficients

$$\alpha_p = \alpha_{wl} + \alpha_{wp} \tag{22}$$

In the above equation α_{wl} is the heat transfer coefficient from the wall to the adjacent liquid layer and α_{wp} is the heat transfer coefficient from the wall to the particles. Following the departure of a particle and of the hot liquid layer, the liquid at T_b from the main body of the fluid flows into the area of influence πd_p^2 and comes into contact with the heating surface at T_w. Assuming pure conduction into the liquid in the area of influence, this can be modelled as conduction to a semi-infinite liquid with a step change in temperature ($\Delta T = T_w - T_b$) at the surface

$$\frac{q_p}{A} = \frac{\sqrt{\lambda\rho c}\,\Delta T}{\sqrt{\pi t}} \tag{23}$$

The hot layer is replaced with a frequency f, which is equal to the frequency of the collision of particles with the heat transfer surface. Hence, similar to the study of Mickic and Rohsenoe [25] on pool boiling, the average heat flux over the area of influence would be:

$$\dot{q}_p = \frac{2\sqrt{\lambda_l\rho_l c_{p,l}}\sqrt{f}\,\Delta T}{\sqrt{\pi}} \tag{24}$$

Taking into account the heat transfer to the particles by conduction when they are in contact with the heat transfer surface, Eq. (24) can be written as

$$\dot{q}_p = \left[\frac{2}{\sqrt{\pi}}\sqrt{\lambda_l\rho_l c_{p,l}} + \left(\frac{\pi d_p^2}{\pi D^2}\right)\sqrt{\lambda_p\rho_p c_{p,p}}\right]\sqrt{f}\,\Delta T \tag{25}$$

Therefore, the heat transfer coefficient for the particle-controlled area can now be obtained from

$$\alpha_p = \left[\frac{2}{\sqrt{\pi}}\sqrt{\lambda_l\rho_l c_{p,l}} + \left(\frac{d_p}{D}\right)^2\sqrt{\lambda_p\rho_p c_{p,p}}\right]\sqrt{f} \tag{26}$$

In the above equations, $\left(\pi d_p^2/\pi D^2\right)$ is dimensionless and taking into account the relative area of contact between particles and heat transfer surface and f is equal to the frequency of particles approaching the heat transfer surface. By analogy to the kinetic theory of gases (applied to the randomly moving solid particles in a fluidized bed) Martin [26,27] has shown that:

$$f = \frac{1}{t_c} = \frac{Cu_p}{4d_p} \tag{27}$$

where C is a constant between 2 and 4 for gas and liquid fluidizations. Determining the particle velocity, u_p in fluidized beds is difficult and would require special equipment. Several investigators, such as Latif and Richardson [28] have speculated that in fluidized beds the particle velocity is proportional to the superficial liquid velocity and that it must be zero at $\varepsilon = \varepsilon_{SB}$. Therefore, it is assumed that

$$u_p = mu_s(\varepsilon - \varepsilon_{SB})^a \tag{28}$$

Considering that particle contact frequency must be zero at $\varepsilon = 1$, and using Eq. (28), Eq. (27) may be modified to:

$$f = K\left(\frac{u_s}{d_p}\right)(\varepsilon - \varepsilon_{SB})^a(1 - \varepsilon)^b \tag{29}$$

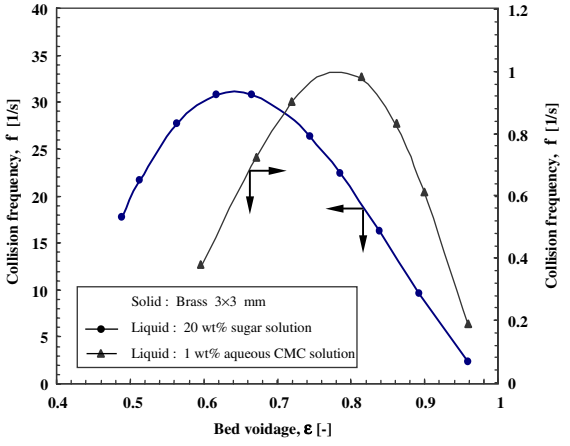

Fig. 5. Collision frequency, f, as a function of bed voidage ε.

in which m, a and b are constants. By analysing a huge number of experimental data (see next paragraph) for both Newtonian and non-Newtonian liquid–solid fluidized beds it was found that for good agreement with experimental data the above equation becomes:

$$f = 1.5\left(\frac{u_s}{d_p}\right)(1-\varepsilon)^{1.8}(\varepsilon-\varepsilon_{SB})^{0.2} \tag{30}$$

In this investigation both particulate and aggregative fluidization behaviour is occurring and from the presented model it is obvious that the heat transfer coefficient depends on the collision frequency of contacting particles, f, according through these equations is related to the bed voidage and hence to the hydrodynamics of the system. The collision frequency of contacting particles with heat transfer surfaces, f, must increase from zero for a packed bed up to a maximum value, at some superficial liquid velocity, before decreasing to zero for single-phase flow.

The collision frequency calculated in the present model (i.e. Eq. (30)) is zero for packed or static beds and for single-phase liquid flow, and generally reaches a maximum for a bed voidage between 0.65 and 0.85, in accordance with the maximum heat transfer coefficient. It is obvious that the contact frequency is affected by the viscosity of the liquid; Fig. 5 shows that it

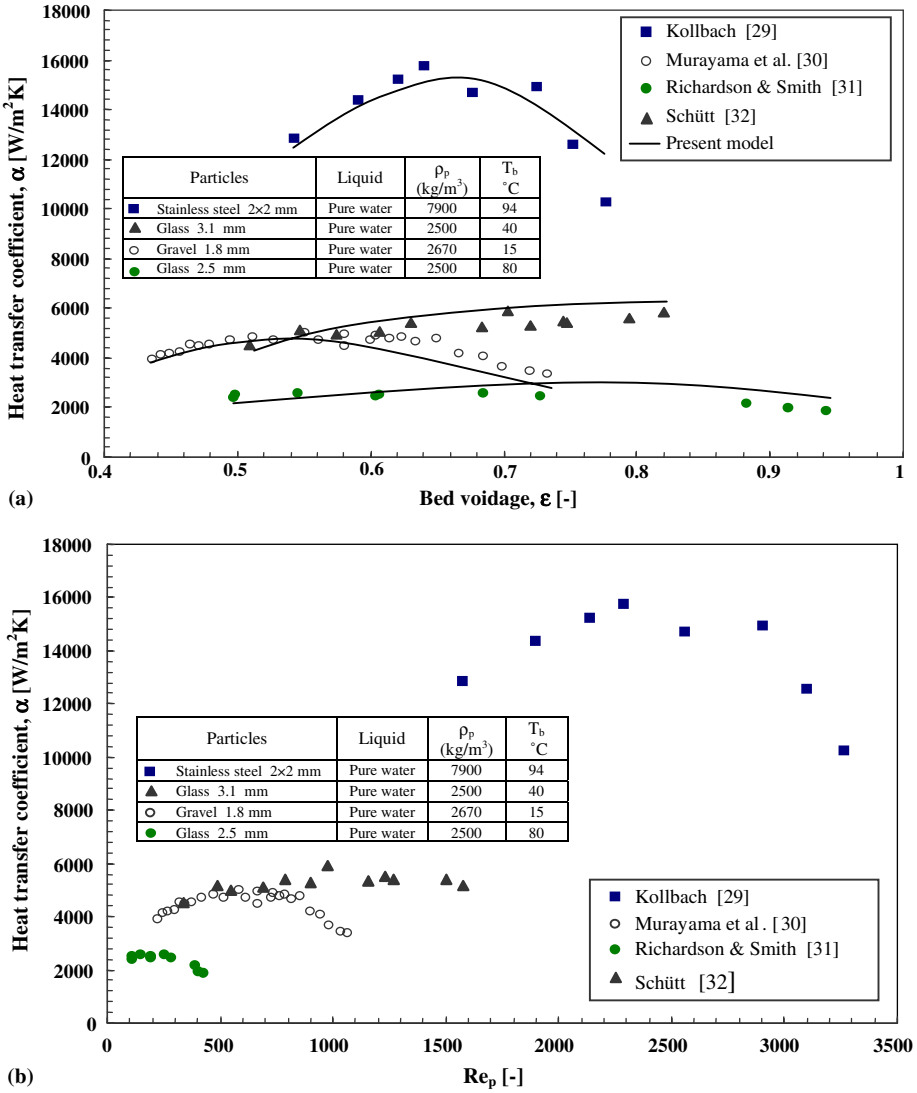

Fig. 6. (a) Comparison of measured and predicted heat transfer coefficients for fluidization in a Newtonian liquid. (b) Heat transfer coefficient as a function of particle Reynolds number for fluidization in Newtonian Liquid.

decreases significantly for fluidization in highly viscous liquids, in which the fluidization behaviour tends to be particulate.

3.6. Comparison of measured heat transfer coefficients with the present model

A large number of data over a wide range of possible operating parameters have been obtained by Aghajani [4] for heat transfer in solid/liquid fluidized beds with Newtonian and non-Newtonian liquids. These data have been complemented by all the published data the authors could extract from the literature. Checking for consistency, all data for velocities greater than the terminal velocity or data sets where the measured wall temperatures were outside the fluidized region were removed. The resulting data bank includes more than 2200 data for Newtonian liquids and more than 800 data points for fluidization with non-Newtonian liquids.

Typical predictions of the present model for different particles fluidized in Newtonian and non-Newtonian solutions are shown in Figs. 6a and 7a. For additional

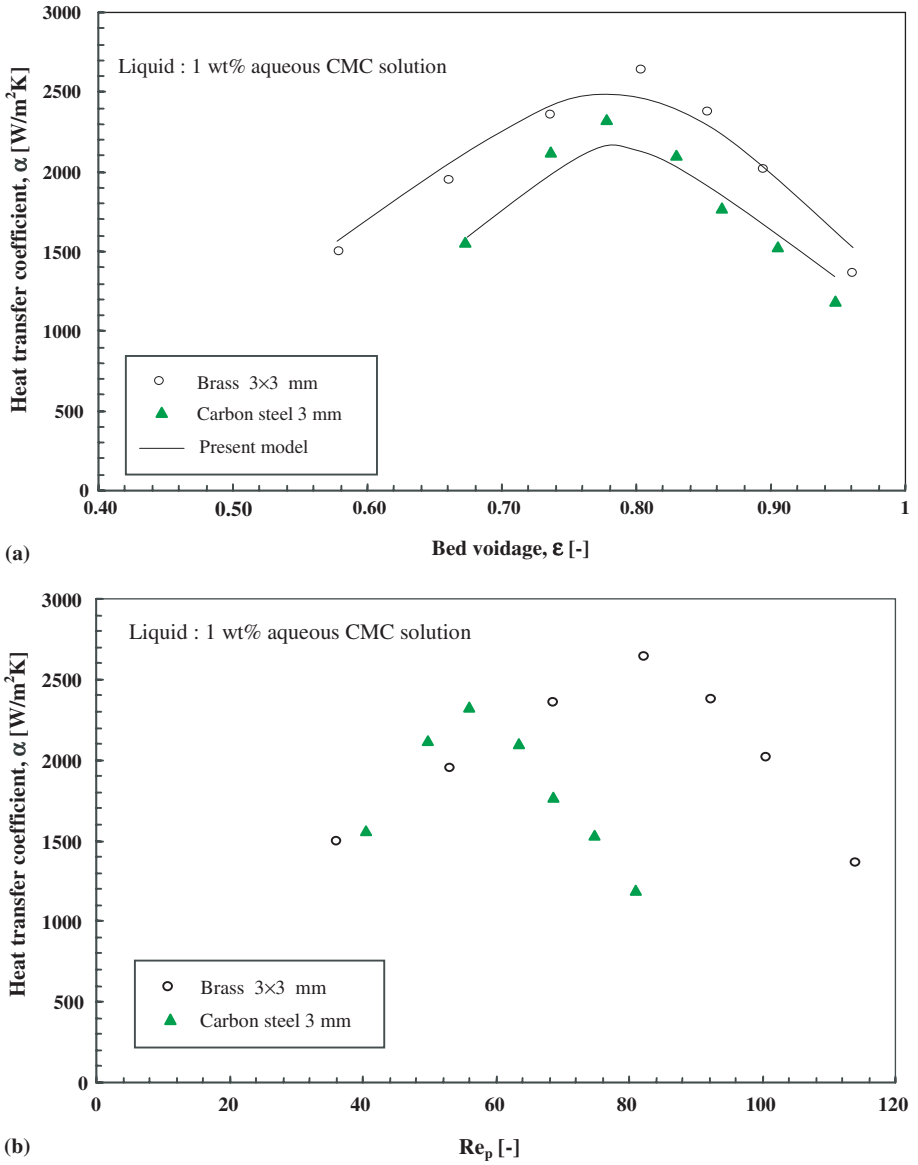

Fig. 7. (a) Comparison of measured and predicted heat transfer coefficients for fluidization in a non-Newtonian liquid. (b) Heat transfer coefficient as a function of particle Reynolds number for fluidization in non-Newtonian Liquid.

information, the same data are plotted as a function of particle Reynolds number in Figs. 6b and 7b. Due to the presence of the suspended solids the heat transfer coefficient increases and reaches a maximum at a bed voidage between 0.6 and 0.8, as shown in Figs. (6a and 7a) for fluidization with Newtonian and non-Newtonian liquids. The calculated trends are in excellent agreement with the experimental data of Aghajani [4] and of all previous investigators. Overall, the average relative error achieved with the present model for heat transfer in solid/liquid fluidized beds was 19.9% for Newtonian and 21.1% for non-Newtonian liquids.

A comparison between calculated and experimental values of heat transfer coefficient was performed for 39 correlations and models listed in Table 4 and also for the present model. More than 2200 data from this study and various publications for solid–liquid fluidized beds with Newtonian liquids and more than 800 data points of the present investigation for solid–liquid fluidized beds with non-Newtonian liquids were used for this

Table 4
Comparison of measured data and values predicted by published models

No.	Author	Newtonian liquids			Non-Newtonian liquids		
		Average relative error (%)	Standard deviation (%)	Prediction	Average relative error (%)	Standard deviation (%)	Prediction
1	Wasser and Mardus [33]	48.8	28.7	–	33	16.4	– –
2	Lemlich and Caldas [34]	94.2	14.2	– –	48.6	20.7	– –
3	Richardson and Mitson [35]	66	36.3	±	652	384	+ +
4	Ruckenstein et al. [36]	59.5	39.5	±	96.3	101	±
5	Richardson and Smith [31]	129.8	152.1	– –	65.2	52.8	+ +
6	Wassmund and Smith [37]	73.8	108.9	±	–	–	–
7	Hamilton [38]	43.7	26.6	±	125.6	83.8	+ +
8	Tripathi and Pandey [39]	70.5	11.2	– –	76.8	7.2	– –
9	Brea and Hamilton [40]	32.8	17.8	±	185	113	+ +
10	Varma et al. [41]	81.5	55.9	– –	–	–	–
11	Schimanski et al. [42]	81.2	10.3	– –	91.5	3.6	– –
12	Syromyatnikov et al. [43]	158.7	114.9	+ +	112.6	103	±
13	Richardson et al. [44]	94.9	65.9	+	163.6	118	++
14	Allen et al. [45]	35.8	19.5	±	89	79	+
15	Baker et al. [46]	80.9	80.2	–	81.5	77.2	±
16	Khan et al. [47]	109	78.4	+ +	189.8	135.6	+ +
17	Tusin et al. [48]	40.4	25.3	– –	61.5	59.4	±
18	Mersman et al. [49]	40.2	24.6	±	125.9	73.3	+ +
19	Kato et al. [50]	36.6	23.2	±	196.3	89.3	+ +
20	Wehrman and Mersmann [51]	42.8	20.4	±	105.6	66.7	+
21	Schütt [52]	46	23.2	±	152.2	93.1	+ +
22	Schütt [32]	46.8	16.9	±	94.2	70.7	+
23	Khan et al. [53]	36.2	24.8	±	53.5	55.7	±
24	Murayama et al. [54]	45.3	32.2	±	45.5	48.2	±
25	Chiu and Ziegler [55]	78.6	16.6	– –	249	126	+ +
26	Juma and Richardson [56]	41.7	19.6	–	44	42.2	±
27	Coulson and Richardson [57]	47.5	35.2	+	98.6	96.1	+
28	Kim et al. [58]	30.7	14.5	–	52.6	57.3	±
29	Midoux et al. [59]	45.3	31.9	+	88.7	55	+
30	Murayama et al. [30]	43	27.3	±	38.2	34.5	±
31	Kollbach [29]	38.6	15.3	±	80.2	58.3	+ +
32	Grewal and Zimmerman [60]	38.1	28	±	138	131	+
33	Kang et al. [61]	38.7	21.5	±	32.2	32.8	±
34	Macias-Machin et al. [62]	47	31.7	– –	88.6	4.4	– –
35	Jamialahmadi and Müller-Steinhagen [5]	35.8	16.3	±	189	216	±
36	Haid et al. [63]	36.7	22.4	±	135.5	83	+ +
37	Jamialahmadi et al. [17]	38.9	17.3	±	127	161	+ +
38	Jamialahmadi et al. [64]	39.3	16.7	±	123	194	+ +
39	Haid [65]	39.7	15.6	±	121	71	+ +
40	Present model	19.9	13.4	±	21.1	16.1	±

analysis. The present model for calculating bed voidage (Eq. (5)), was used to predict the bed voidage.

The average relative errors $|\Delta_{rel}\alpha|_{av}$ and the standard deviation of prediction, σ, of all correlations used in this comparison, which are defined as follows, are shown in Table 4.

Relative error,

$$|\Delta_{rel}\alpha| = \left|(\alpha_{cal} - \alpha_{exp})/\alpha_{exp}\right|(\%)$$

Average relative error,

$$|\Delta_{rel}\alpha|_{av} = \sum |\Delta_{rel}\alpha| \, /n(\%),$$

n = number of data sets

Standard deviation,

$$\sigma = \left(\sum(|\Delta_{rel}\alpha| - |\Delta_{rel}\alpha|_{av})^2/n\right)^{0.5}(\%),$$

n = number of data sets

Comparing the average relative errors and the standard deviation of predicted values for all published correlations and of the present model, it is evident that the model developed in the present investigation provides better results than all other correlations. This table also indicates whether correlations tend to underpredict "−" or overpredict "+" the measurements. Correlations with "−− " or "++" have a high tendency to underpredict or overpredict the measurements, and for correlations with "±" no clear tendency was found.

4. Conclusions

New models are presented for bed voidage and heat transfer coefficients for solid/liquid fluidized beds in vertical pipes. These mechanistic models take into consideration the forces acting on the particles as well as the interaction between heat transfer surface and fluidized particles. They are applicable for both Newtonian and non-Newtonian liquids. Comparison with two substantial data banks with data from various authors indicates that the two models outperform previously published correlations.

References

[1] M. Jamialahmadi, H. Müller-Steinhagen, Hydrodynamics and heat transfer of liquid fluidized bed systems, Chem. Eng. Comm. 179 (2000) 35–79.
[2] H.M. Müller-Steinhagen, Laboratory and pilot plant measurements for fouling reduction with liquid/solid fluidized bed, in: United Engineering Foundation Conference on Heat Exchanger Fouling Santa Fé., 2003.
[3] D.G. Klaren, The fluid bed heat exchanger: principles and modes of operation and heat transfer results under sever fouling condition, Fouling Prev. Res. Dis. 5 (1) (1983).
[4] M. Aghajani, Studies of Bed Voidage and Heat Transfer in Solid–Liquid Fluidized Bed Heat Exchangers, PhD thesis, University of Surrey, UK, 2001.
[5] M. Jamialahmadi, H. Müller-Steinhagen, Bed voidage in annular solid–liquid fluidized beds, Chem. Eng. Process. 31 (1992) 221–227.
[6] R.H. Wilhelm, M. Kwauk, Fluidization of solid particles, Chem. Eng. Progress 4 (1948) 347–352.
[7] W.K. Lewis, E.R. Gililand, W. Bauer, Characteristics of fluidized particles, Ind. Eng. Chem. 41 (1949) 1104–1117.
[8] J.F. Richardson, W.N. Zaki, Sedimentation and fluidization: Part I, Trans. Instn. Chem. Engrs. 32 (1954) 35–53.
[9] J. Happel, Viscous flow in multiparticle systems: slow motion of fluids relative to beds of spherical particles and particulate fluidization and sedimentation of spheres, AIChE J. 4 (1958) 197–201.
[10] D.L. Strauve, L. Lapidus, J.C. Elgin, The mechanics of moving vertical fluidized systems, Can. J. Chem. Eng. 36 (1958) 141–152.
[11] A.L. Loeffler, B.F. Ruth, Particulate fluidization and sedimentation of spheres, AIChE J. 5 (1959) 310–315.
[12] C.Y. Wen, Y.H. Yu, Mechanism of fluidization, Chem. Eng. Progress Sympos. Series 44 (1966) 201–218.
[13] E. Barnea, J. Mizrahi, A generalized approach to the fluid dynamics of particulate systems. Part 1: general correlation for fluidization and sedimentation in solid multiparticle systems, Chem. Eng. J. 5 (1973) 171–189.
[14] J. Garside, M.R. Al-Dibouni, Velocity–voidage relationships for fluidization and sedimentation in solid–liquid systems, Ind. Eng. Chem. Process Des. Dev. 16 (1977) 206–213.
[15] A. Hirata, F.B. Bulos, Predicting bed voidage in solid–liquid fluidization, J. Chem. Eng. Jpn. 23 (1990) 599–604.
[16] M. Hartman, D. Tmka, V. Havlin, A relationship to estimate the porosity in liquid–solid fluidized beds, Chem. Eng. Sci. 47 (12) (1992) 3162–3166.
[17] M. Jamialahmadi, M.R. Malayeri, H. Müller-Steinhagen, Prediction of heat transfer to liquid–solid fluidized beds, Can. J. Chem. Eng. 73 (1995) 444–455.
[18] R. Letan, On vertical dispersion two-phase flow, Chem. Eng. Sci. 29 (1974) 621–624.
[19] R. Clift, J.R. Grace, M.E. Weber, Bubbles, Drops and Particles, Academic Press, New York, 1978.
[20] A.R. Khan, J.F. Richardson, The resistance to motion of a solid sphere in a fluid, Chem. Eng. Commun. 62 (1987) 135–147.
[21] M. Hartman, D. Tmka, V. Havlin, A relationship to estimate the porosity in liquid–solid fluidized beds, Chem. Eng. Sci. 47 (1992) 3162–3166.
[22] C.Y. Han, P. Griffith, The mechanism of heat transfer in nucleate pool boiling, Part I and II, Int. J. Heat Mass Transfer 8 (1965) 887–917.
[23] V. Gnielinski, Wärmeübergang in Rohren, VDI-Wärmeatlas, fifth ed., VDI-Verlag, Düsseldorf, 1986.
[24] G.K. Filonenko, Hydraulic resistance in pipes, Teploenergetika 1 (1954) 40–44.
[25] B.B. Mickic, W.M. Rohsenoe, A new correlation of pool boiling data including the effect of heat surface characteristics, J. Heat Transfer 5 (1969) 245–250.

[26] H. Martin, Heat transfer between gas fluidized bed of solid particles and the surfaces of immersed heat exchanger elements, Part II, Chem. Eng. Process 18 (1984) 199–223.
[27] H. Martin, Fluid bed heat exchangers—A new model for particle convection energy transfer, Chem. Eng. Commun. 13 (1981) 1–16.
[28] B.A.J. Latif, J.F. Richardson, Circulation patterns and velocity distributions for particles in a liquid fluidized bed, Chem. Eng. Sci. 72 (1972) 1933–1949.
[29] J. Kollbach, PhD Thesis, Universität Achen, Achen, 1987.
[30] K. Murayama, M. Fuluma, A. Yasunishi, Wall-to-bed heat transfer in liquid–solid and gas–liquid–solid fluidized beds, Can. J. Chem. Eng. 64 (1986) 399–408.
[31] J.F. Richardson, J.W. Smith, Heat transfer to liquid-fluidized systems and to suspensions of coarse particles in vertical transport, Trans. Inst. Chem. Eng. 40 (1962) 13–22.
[32] U. Schütt, Wärmeübertragung in der Flüssigkeitswirbelschicht mit senkrechten Rohren, Ph.D. Thesis, Universität Magdeburg, 1983.
[33] U. Wasser, G. Mardas, Zum Wärmeübergang in Wirbelschichten, Chem. Ing. Techn. 29 (1957) 332–335.
[34] R. Lemlich, I. Caldas, Heat transfer to liquid fluidized bed, AIChE J. 4 (1958) 376–380.
[35] J.F. Richardson, A.E. Mitson, Sedimentation and fluidization. Part II—Heat transfer from a tube wall to a liquid-fluidized system, Trans. Inst. Chem. Eng. 36 (1958) 270–282.
[36] E. Ruckenstein, V. Shorr, G. Suciu, Despre Transferul de Caldurs Dintre un Strat Fluidizat Culichid si PeretelevasuluiCare-I Contine, Studdi Cercetari Fizica, Akad. Rep. Populare Romine 10 (1959) 235.
[37] B.W. Wassmund, J.W. Smith, Wall to fluid heat transfer in liquid fluidized beds, Can. J. Chem. Eng. 45 (1967) 156–165.
[38] W. Hamilton, A correlation for heat transfer in liquid fluidized beds, Can. J. Chem. Eng. 48 (1970) 52–55.
[39] G. Tripathi, G.N. Pandey, Heat transfer in liquid fluidized beds, Indian J. Technol. 8 (1970) 285–289.
[40] F.M. Brea, W. Hamilton, Heat transfer in liquid fluidized beds, Trans. Inst. Chem. Eng. 49 (1971) 196–203.
[41] R.L. Varma, C.N. Pandey, G. Tripathy, Heat transfer in semifluidized beds, Indian J. Technol. 10 (1972) 11–15.
[42] G.N. Schimanski, E.N. Jancuk, P.G. Nikitin, Untersuchung der Wärmeübertragung Zwischen einem Waagerechten Rohrbündel und einer Wirbelschicht, Arch. Energiewirt. 27 (1972) 25–29.
[43] N.I. Syromyatnikov, L.K. Vasanora, A.I. Karpenko, Heat transfer in liquid fluidized bed, Heat Transfer Sov. Res. 6 (1973) 135–139.
[44] J.F. Richardson, M.N. Romani, K.J. Shakiri, Heat transfer from immersed surfaces in liquid fluidized beds, Chem. Eng. Sci. 31 (1976) 619–624.
[45] C.A. Allen, O. Fukuda, E.S. Grimmett, R.E. Mc Atee, Liquid fluidized bed heat exchanger-horizontal configuration experiments and data correlations, in: 12th Intersociety Energy Conversion Engineering Conference, Preprints, 1977, pp. 831–838.
[46] C.G.J. Baker, E.R. Armstrong, M.A. Bergougnou, Heat transfer in three-phase fluidized beds, Powder Technol. 21 (1978) 195–204.
[47] A.R. Khan, J.F. Richardson, K.J. Shakiri, Heat Transfer Between a Fluidized Bed and a Small Immersed Surface, Cambridge University Press, 1978, pp. 351–356.
[48] A.M. Tusin, L.K. Vasanova, N.J. Syromyatnikov, Heat transfer from a transverse streamlined cylinder during surface boiling in a liquid fluidized bed, J. Eng. Phys. 32 (1979) 263–266.
[49] A. Mersman, H. Noth, O. Ringer, R. Wunder, Maximaler Wärmeübergang in Apparaten mit Dispersen Zweiphasensystemen, Chem. Ing. Tech. 52 (1980) 189–198.
[50] Y. Kato, T. Kago, K. Uchida, S. Morroka, Liquid hold-up and heat transfer coefficient between bed and wall in liquid–solid and gas–liquid–solid fluidized beds, Powder Technol. 28 (1981) 173–179.
[51] M. Wehrman, A. Mersmann, Wärmeübergang in flüssigkeits durchströmten Fest und fliess betten, Chem. Ing. Techn. 53 (1981) 804–805, Ms 940/81.
[52] U. Schütt, Wärmeübertragung in der Flüssigkeitswirbelschicht mit senkrechten Rohren, Wiss Zeitung Techn. Hochschule Magdeburg 26 (1982) 71–74.
[53] A.R. Khan, K.A. Juma, J.F. Richardson, Heat transfer from a plane surface to liquids and liquid–solid fluidized beds, Chem. Eng. Sci. 38 (1983) 2053–2066.
[54] K. Murayama, M. Fuluma, A. Yasunishi, Wall-to-bed heat transfer in gas–liquid–solid fluidized beds, Can. J. Chem. Eng. 62 (1984) 199–208.
[55] T.M. Chiu, E.N. Ziegler, Liquid hold-up and heat transfer coefficient in liquid–solid and three-phase fluidized bed, AIChE J. 31 (1985) 1504–1509.
[56] A.K.A. Juma, J.F. Richardson, Heat transfer to cylinders from segregating liquid–solid fluidized beds, Chem. Eng. Sci. 40 (1985) 687–694.
[57] J.M. Coulson, J. Richardson, Chemical Engineering, vol. 2, third ed., Pergamon Press, Oxford, 1985.
[58] S.D. Kim, Y. Kang, H.K. Kwon, Heat transfer characteristics in two and three phase slurry fluidized beds, AIChE J. 32 (1986) 1397–1400.
[59] N. Midoux, J. Wild, M. Purwasamita, J.C. Chapentier, H. Martin, Zum Flüssigkeitsinhalt und zum Wärmeübergang in Rieselbettreaktoren bei boher Wechselwirkung des Gases und der Flüssigkeit, Chem. Eng. Tech. 58 (1986) 142–143, MS1445/86.
[60] N.S. Grewal, A.T. Zimmerman, Heat transfer from tube immersed in a liquid–solid fluidized bed, Powder Technol. 54 (1988) 137–145.
[61] Y. Kang, L.T. Fan, S.D. Kim, Immersed heater-type bed heat transfer in liquid–solid fluidized beds, AIChE J. 37 (1991) 1101–1106.
[62] A. Macias-Machin, L. Oufer, N. Wannenmacher, Heat transfer between an immersed wire and a liquid fluidized bed, Powder Technol. 66 (1991) 281–284.
[63] M. Haid, H. Martin, H. Müller-Steinhagen, Heat transfer to liquid–solid fluidized beds, Chem. Eng. Process. 33 (1994) 211–225.
[64] M. Jamialahmadi, M.R. Malayeri, H. Mülller-Steinhagen, A unified correlation for the prediction of heat transfer coefficients in liquid–solid fluidized bed systems, J. Heat Transfer 118 (1996) 952–959.
[65] M. Haid, Correlations for the prediction of heat transfer to liquid–solid fluidized beds, Chem. Eng. Process. 36 (1997) 143–147.